that have been implicated in many bacterial, mycobacterial, fungal, and parasitic diseases (*9*). There are two models for the development of T_H1 and T_H2 responses: the first suggests that they derive from distinct precursors (*10*), whereas the second suggests that they arise from a common lineage. The use of peptide-specific clones (*11*), limiting dilution analysis (*12*), and transgenic mice expressing a single TCR (*13*) support the second possibility, and the findings in this paper extend these previous observations by linking subset maturation to biologically important antigens implicated in the immune response to an infectious organism.

Evidence supporting an oligoclonal immune response was obtained by flow cytofluorometric analysis, direct sequencing of receptors from parasite-specific $CD4^+$ T cell clones, and amplification of genomic rearrangements as extracted from infected mice. The response had unusual features. First, several of the clones used common variable region genes but expressed distinct junctional sequences. The junctional diversity created by N region additions and exonucleotytic nibbling generates the CDR3 domain of the TCR implicated in the interaction with peptide (*14*). Although this implies that these different clones should recognize distinct epitopes, instances in which conserved V regions seem to contribute substantially to fine specificity despite CDR3 differences have been noted (*15*). Second, 90% of the deduced junctional sequences of the *Leishmania*-specific clones contain anionic residues in this region (*16*), perhaps indicating recognition of a cationic parasite antigen (*17*). The importance of charged residues within the CDR3 domain in shaping the TCR-peptide interaction with MHC has been delineated with the use of transgenic mice expressing single-chain TCRs (*18*). Third, the occurrence of relatively conserved TCR sequences among different animals and across MHC class II boundaries was not predicted. The generation of the rearranged functional TCR is not random; bias in the use of junctional nucleotide additions contributes to constraints on CDR3 length (*19*). The frequent use of the $V_\alpha8$-J_αTA72 rearrangement suggests that the CDR3 region of the TCRα chain may interact with a monomorphic parasite determinant, whereas the variation in pairing with $V_\beta4$ or in the $V_\beta4$-D-J_β recombination may provide the necessary polymorphism to bind different MHC molecules.

The nature of the antigen constitutes an important area for further investigation. Experiments to date have identified reactivity in association with a 10-kD protein that stimulates the protective BALB/c-derived clone, 9.1-2 (*8*). The identification of this antigen in all *Leishmania* species analyzed (*8*) is consistent with its important role in the immune response and in disease. As shown in the present study, however, the immunologic milieu, rather than the antigen, may be more important in determining the development of a successful immune response. A search for factors that modify the developmental regulation of $CD4^+$ subsets might ultimately be more productive than the hope that universally protective microbial antigens can be reliably identified.

REFERENCES AND NOTES

1. F. P. Heinzel *et al.*, *Proc. Natl. Acad. Sci. U.S.A.* **88**, 7011 (1991); F. P. Heinzel *et al.*, *J. Exp. Med.* **169**, 59 (1989).
2. M. Lehn *et al.*, *J. Immunol.* **143**, 3020 (1989); C. Bogdan *et al.*, *J. Exp. Med.* **174**, 1549 (1991); R. de Waal Malefyt *et al.*, *ibid.*, p. 915.
3. R. G. Titus, R. Ceredig, J.-C. Cerottini, J. A. Louis, *J. Immunol.* **135**, 2108 (1985).
4. M. D. Sadick *et al.*, *J. Exp. Med.* **171**, 115 (1990).
5. B. J. Holaday *et al.*, *J. Immunol.* **147**, 1653 (1991); P. Scott, P. Natovitz, R. L. Coffman, E. Pearce, A. Sher, *J. Exp. Med.* **168**, 1675 (1988).
6. M. Belosevic *et al.*, *J. Immunol.* **143**, 266 (1989); R. Chatelain, K. Varkila, R. L. Coffman, *ibid.* **148**, 1182 (1992).
7. We selected clones 9.1-2 and H27 and U2, U3, and U4 by limiting dilution from characterized *Leishmania*-specific T_H1 and T_H2 $CD4^+$ cell lines that adoptively transfer protection or exacerbation, respectively (*5*). Clone 9.1-2 is a protective $CD4^+$ clone derived from an immunized BALB/c mouse (*8*). The remaining TCR sequences were generated from hybridomas established by fusion of $CD4^+$ lymph node cells from healing (that is, previously treated with anti-CD4) BALB/c mice or BALB/c mice with progressive infection with the TCRα- and TCRβ-negative mutant thymoma cell line, BW 5147 1100.129.237 (*20*). Viable clones were selected for analysis only if they expressed CD4 and TCR, as assessed by fluorescence analysis, and released either IFN-γ or IL-4 in response to stimulation with a sonicate of *Leishmania* antigen plus antigen-presenting cells. The cytokine response was only transiently expressed in these hybridomas but permitted the assignment of one-third of the viable hybridomas to a T_H1 or T_H2 phenotype.
8. P. Scott, P. Caspar, A. Sher, *J. Immunol.* **144**, 1075 (1990).
9. G. Del Prete *et al.*, *J. Clin. Invest.* **88**, 346 (1991); H. Yssel *et al.*, *J. Exp. Med.* **174**, 593 (1991); J. B. A. G. Haanen *et al.*, *ibid.*, p. 583; M. Yamamura *et al.*, *Science* **254**, 277 (1991); P. Salgame *et al.*, *ibid.*, p. 279; L. Romani *et al.*, *J. Exp. Med.* **176**, 19 (1992); A. Sher and R. L. Coffman, *Annu. Rev. Immunol.* **10**, 385 (1992).
10. N. E. Street and T. R. Mosmann, *FASEB J.* **5**, 171 (1991).
11. B. D. Evavold *et al.*, *J. Immunol.* **148**, 347 (1992).
12. M. Rocken, J.-H. Saurat, C. Hauser, *ibid.*, p. 1031.
13. R. A. Seder, W. E. Paul, M. M. Davis, B. F. de St. Groth, *J. Exp. Med.* **176**, 1091 (1992).
14. J. L. Jorgensen, P. A. Reay, E. W. Ehrich, M. M. Davis, *Annu. Rev. Immunol.* **10**, 835 (1992).
15. B. Boitel *et al.*, *J. Exp. Med.* **175**, 765 (1992); J.-L. Casanova, P. Romero, C. Widmann, P. Kourilsky, J. L. Maryanski, *ibid.* **174**, 1371 (1991).
16. S. L. Reiner, unpublished data.
17. S. Adams, P. LaBlanc, S. K. Datta, *Proc. Natl. Acad. Sci. U.S.A.* **88**, 11271 (1991).
18. J. L. Jorgensen *et al.*, *Nature* **355**, 224 (1992).
19. S. Candeias, C. Waltzinger, C. Benoist, D. Mathis, *J. Exp. Med.* **174**, 989 (1991).
20. J. White *et al.*, *J. Immunol.* **143**, 1822 (1989).
21. K. Tomonari, E. Lovering, S. Fairchild, S. Spencer, *Eur. J. Immunol.* **19**, 1131 (1989).
22. K. Tomonari, E. Lovering, S. Spencer, *Immunogenetics* **31**, 333 (1990).
23. Y. Choi *et al.*, *Proc. Natl. Acad. Sci. U.S.A.* **86**, 8941 (1989).
24. A. H. Taylor, A. M. Haberman, W. Gerhard, A. J. Caton, *J. Exp. Med.* **172**, 1643 (1990).
25. H. S. Chou *et al.*, *EMBO J.* **5**, 2149 (1986).

26. We thank M. Sadick and B. Holaday for providing T cell clones; O. Kanegawa, F. Fitch, D. Loh, J. Kappler, P. Marrack, K. Wang, L. Hood, I. Weissman, and G. Fathman for reagents; N. Killeen, A. Theofilopoulos, and A. Caton for technical advice; and D. Littman, A. DeFranco, and J. Boothroyd for critical comments. Supported by NIH grant AI30663 and the Burroughs Wellcome Fund.

7 October 1992; accepted 11 January 1993

Inhibition of Human Colon Cancer Growth by Antibody-Directed Human LAK Cells in SCID Mice

Hiroshi Takahashi,* Tetsuya Nakada, Isabelle Puisieux

Advanced human colon cancer does not respond to lymphokine-activated killer (LAK) cells. In order to direct cytotoxic cells to the tumor, human LAK cells linked with antibodies to a tumor cell surface antigen were tested with established hepatic metastases in severe combined immunodeficient (SCID) mice. These cells had increased uptake into the tumor and suppression of tumor growth as compared with LAK cells alone, thereby improving the survival of tumor-bearing mice. Thus, tumor growth can be inhibited by targeted LAK cells, and SCID mice can be used to test the antitumor properties of human effector cells.

Lymphokine-activated killer cells generated by interleukin-2 (IL-2) are cytotoxic to colon cancer cells in vitro (*1*). However, in clinical trials, advanced human colon cancer has been refractory to adoptive immunotherapy using LAK cells (*2*). This limitation of LAK therapy may be due in part to an ineffectiveness of LAK cell cytotoxicity (*3*) or a lack of recruitment of LAK cells to the tumor mass (*4*). In this report, we demonstrate that human LAK cells can be targeted to the tumor by antibodies to a tumor cell surface antigen. This targeting augments the LAK cell effectiveness against hepatic metastases of human colon cancer in SCID mice (*5*).

SCID mice have no functional T and B cells and therefore will not reject xenografts

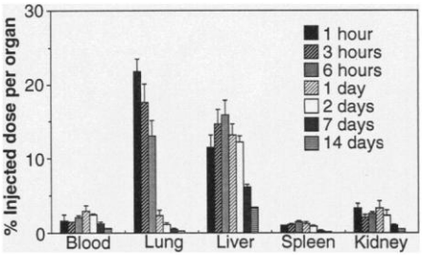

Fig. 1. Biodistribution of human LAK cells in SCID mice. C.B-17 SCID mice were purchased from Taconic (Germantown, New York). All animal experiments were approved by the committee on research animal care protocol review group and carried out according to Massachusetts General Hospital guidelines. Mononuclear cells were isolated from healthy volunteers by gradient density centrifugation and incubated in the plastic plate coated with fibronectin to prepare adherent cell-free human PBLs. LAK cells were generated by incubation of these PBLs with recombinant human IL-2 (100 U/ml; Shionogi Pharmaceutical Co., Osaka, Japan) for 48 hours at 37°C. The biodistribution was examined by intravenous injection of human LAK cells labeled with [^{3}H]uridine and human IL-2 (500 U per mouse) into SCID mice. The radioactivity of each organ was examined after tissues were digested by Solvable (Du Pont) and was expressed as the percentage of injected dose per organ. Three animals were used to determine each value (mean ± SD).

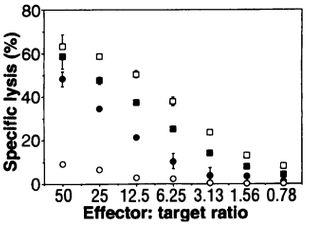

Fig. 2. Cytotoxicity produced by human PBLs and LAK cells conjugated to MAb c-SF-25. Circles, PBLs; squares, LAK cells; empty symbols, cells alone; filled symbols, cells conjugated to c-SF-25. Cytotoxicity was assessed by 4-hour ^{51}Cr-release assay with LS 180 cells as targets at different effector/target cell ratios (E/T ratio) (*21*). Results are the mean ± SD of values obtained in triplicate experiments. Although PEG treatment did not affect the viability of effector cells, it was slightly detrimental to LAK cell cytotoxicity.

of human lymphocytes or human tumors (*5*). These mice can be repopulated with human T or B cells, and human tumors with infiltrating lymphocytes have been propagated (*6*). SCID mice have been used to examine the growth of human lymphoma cells after exposure to cytokine-activated human killer cells in vitro (*7*). However, the use of the SCID mouse model to test the antitumor effects of exogenous human effector cells by intravenous administration has not been established. The short-term survival and biodistribution of human LAK cells labeled with [^{3}H]uridine was examined in SCID mice after intravenous injection (Fig. 1). Human LAK cells were detectable up to 14 days, and most cells were in the liver after being temporarily trapped in the lung.

Injection of LS 180 human colon adenocarcinoma cells into the portal vein via the spleen of SCID mice establishes in these mice a model for human colon cancer (*8, 9*). Although this animal model does not represent all the steps of the metastatic cascade (*10*), it simulates the metastatic growth of tumor cells in the liver after vascular spread. All mice eventually die from extensive hepatic parenchymal involvement of tumors within 6 to 7 weeks after tumor cell injection.

Although tumor-specific antibodies may be useful for targeting cytotoxic effector cells to tumor cells, it is not clear whether in vivo immunolocalization is improved (*11*). The monoclonal antibody (MAb) SF-25 recognizes a 125-kD cell surface antigen (K_a = 2.36 × 10^9 M^{-1}) that is expressed on human colon adenocarcinomas (*12*). MAb SF-25 injected intravenously immunolocalizes to human colon adenocarcinomas previously established in the liver of nude mice (*8*). The MAb SF-25 alone does not inhibit tumor cell growth in vitro, and SF-25 antigen is neither internalized nor shed from the tumor cell surface (*13*). We used MAb SF-25 to augment LAK cell effectiveness.

The immunological defect of SCID mice is limited to a stem cell progenitor of T and B lymphocytes (*5*); macrophage and natural killer (NK) cell functions are intact (*14*). Therefore, such effector cell populations might inhibit tumor growth through interactions with injected antibodies (*15*). To assess if MAb SF-25 would augment the in vivo antitumor effect of human LAK cells without interfering with the murine immune system in this animal model, we linked a modified MAb SF-25 to human LAK cells with polyethylene glycol (PEG) (*16*). We used a recombinant chimeric antibody construct of MAb SF-25 (MAb c-SF-25) that has the variable region of murine MAb SF-25 and constant region of human immunoglobulin (Ig) G1 (*17*). Most LAK cells express an Fc receptor for IgG (FcγR type III) (CD16) (*1, 18*), and human IgG1 binds to this FcγR (*19*). Therefore, the antigen-combining site of MAb c-SF-25 is more likely to be exposed in an outward orientation because the Fc region should bind to FcγR on the cell surface of LAK cells. PEG treatment then enhances the binding of MAb to LAK cells. Ten times more antibodies were conjugated to LAK cells by PEG treatment than by incubation with the MAb c-SF-25 alone (~0.1 and 0.01 pmol of MAb per 10^7 LAK cells, respectively) (*20*).

The availability of the antigen-combining site to bind with target cells was examined with the use of a cytotoxicity assay of macrophage-depleted human peripheral blood lymphocytes (PBLs); NK cells in human PBLs express FcγR type III and initiate antibody-dependent cell-mediated cytotoxicity (ADCC) on binding to the antibody (*21*) (Fig. 2). Human PBLs conjugated to MAb c-SF-25 (c-SF-25-PBL) were cytotoxic toward LS 180 cells. In contrast, human PBLs alone under the same conditions were not. The ADCC response requires simultaneous binding of the antigen-combining site of an antibody with the antigen and the Fc region to FcγRs on the effector cell (*21*). Therefore, MAb c-SF-25 is functionally available to bind to LS 180 tumor cells after conjugation of the antibody to cells. Human LAK cells with and without conjugated c-SF-25 were cytotoxic (Fig. 2). However, when these c-SF-25-LAK cells were labeled with [^{3}H]uridine and injected into the SCID–human colon cancer model, increased uptake into the tumor site was observed (Table 1). Tumor uptake of c-SF-25-LAK was about three times higher than that of LAK cells alone,

Table 1. Tumor uptake of LAK cells conjugated to MAb c-SF-25.

	Percentage of injected dose per gram of tissue*					
	3 hours†		6 hours		24 hours	
c-SF-25-LAK	6.24 ± 0.22	0.6517‡	26.22 ± 4.98	0.0061	22.19 ± 1.36	0.0001
LAK alone	5.09 ± 2.70		8.91 ± 3.51		6.57 ± 0.73	

*Human LAK cells were labeled with [^{3}H]uridine and intravenously injected into SCID mice bearing LS180 hepatic metastases. Tumor uptake was determined by measurement of radioactivity in tumors dissected from surrounding normal liver and was expressed as the percentage of injected dose per gram of tumor tissue. Two to four animals were used to determine each value (mean ± SD). †Hours after intravenous injection of [^{3}H]uridine-labeled effector cells. ‡Statistical significance was examined by two-sided Student's unpaired *t* test.

Molecular Hepatology Laboratory, Massachusetts General Hospital Cancer Center, Charlestown, MA 02129, and Department of Medicine, Harvard Medical School, Boston, MA 02115.

*To whom correspondence should be addressed at Molecular Hepatology Laboratory, Massachusetts General Hospital Cancer Center, Charlestown, MA 02129.

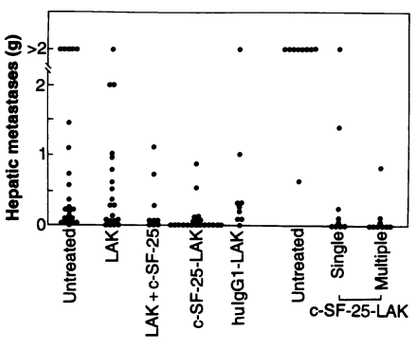

Fig. 3. Tumor growth after c-SF-25-LAK treatment. Tumors were carefully separated from surrounding normal liver after formaldehyde fixation and evaluated by an independent investigator (M. Nakaki). A vertical axis denotes the weight of hepatic metastases. The differences in tumor weights were tested by Kruskal-Wallis statistic followed by Mann-Whitney rank sum test with Bonferroni correction to conduct multiple comparisons. The effect of different treatments (Kruskal-Wallis test, $P = 0.0011$) is given as follows: untreated mice versus mice treated with LAK cells alone (LAK), LAK cells incubated with c-SF-25 without PEG treatment (LAK + c-SF-25), c-SF-25-LAK, or LAK cells conjugated to human IgG1 isolated from myeloma plasma (huIgG1-LAK) ($P = 0.5755$, $P = 0.0749$, $P = 0.0002$, and $P = 0.9165$, respectively); c-SF-25-LAK versus LAK, LAK + c-SF-25, or huIgG1-LAK ($P = 0.0020$, $P = 0.2783$, and $P = 0.0040$, respectively). The statistically significant α level is $0.05/7 = 0.0071$. The effect of multiple injections of c-SF-25-LAK cells (Kruskal-Wallis test, $P = 0.0005$) is given as follows: untreated mice versus mice receiving single or multiple injections ($P = 0.0030$ and $P = 0.0005$, respectively) and multiple versus single injections ($P = 0.9840$). The statistically significant α level is $0.05/3 = 0.0167$. Most of the mice treated with c-SF-25-LAK were free of detectable hepatic metastasis.

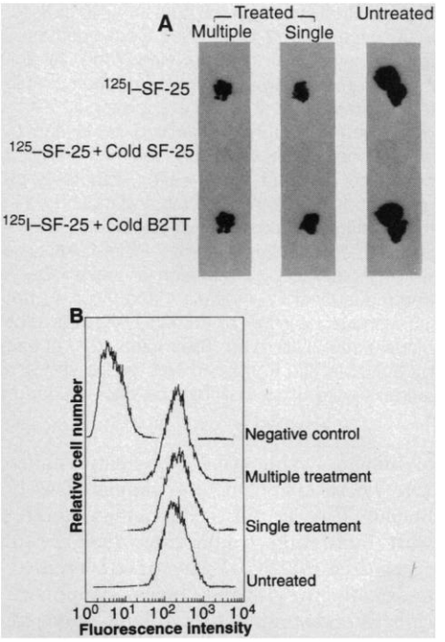

Fig. 4. Expression of SF-25 antigen in LS 180 tumor after treatment with c-SF-25-LAK. (**A**) Histological examination of SF-25 antigen. The cryostat sections of hepatic metastases derived from treated (single or multiple injection of c-SF-25-LAK cells) or untreated SCID mice were incubated with ^{125}I-labeled MAb SF-25 and autoradiographed as described (*8*). SF-25 antigen was highly expressed in both c-SF-25-LAK–treated and untreated tumors as shown by the dense and homogenous radioactive spots. This reaction was specific because it was inhibited only by unlabeled specific antibody and not by an irrelevant MAb (B2TT) to tetanus toxoid. (**B**) Flow cytometric analysis of SF-25 antigen. A single cell suspension of LS 180 cells was prepared from hepatic tumors derived from the c-SF-25-LAK–treated (single or multiple) and untreated mice. The expression of SF-25 antigen at the cellular level was examined by flow cytometry with the use of fluorescein isothiocyanate (FITC)–labeled MAb SF-25. FITC-labeled irrelevant MAb (B2TT) served as a negative control. The antigen was uniformly expressed at high density in most of the cell populations (>99%) from both untreated and treated mice.

and the increased uptake was statistically significant (Table 1).

Five days after the injection of LS 180 cells into the portal vein and when micrometastatic disease was present, c-SF-25-LAK cells, LAK cells alone, LAK cells incubated with MAb c-SF-25 without PEG treatment (*20*), or human IgG1-LAK cells were injected intravenously into SCID mice [10^7 cells with 500 U of IL-2 in 200 μl of phosphate-buffered saline (PBS) per mouse, respectively] (Fig. 3). The weight of hepatic tumor masses from each mouse was determined 5 weeks after tumor cell injection; that of untreated mice was 1.07 ± 1.60 g (mean ± SD, $n = 23$). A single intravenous injection of c-SF-25-LAK cells substantially inhibited the tumor growth (0.08 ± 0.23 g, $n = 20$). In contrast, human LAK cells alone, LAK cells incubated with c-MAb SF-25, and human IgG1-LAK cells were less effective (0.58 ± 0.76 g, $n = 20$; 0.25 ± 0.41 g, $n = 9$; and 0.54 ± 0.80 g, $n = 9$, respectively). The decrease in tumor weight was statistically significant only in the c-SF-25-LAK–treated group as compared with the untreated group. The anti-tumor effect of multiple injections was also examined by the injection of c-SF-25-LAK cells once weekly for three consecutive weeks. Inhibition of tumor growth was more prominent with multiple injections (untreated mice, 2.76 ± 1.12 g, $n = 9$; single injection, 0.51 ± 0.95 g, $n = 9$; and multiple injections, 0.11 ± 0.27 g, $n = 9$).

The duration of survival of SCID mice injected with c-SF-25-LAK cells (10^7) 7 days after the tumor cell injection was determined. All untreated mice died within 7 weeks after tumor cell injection as a result of massive parenchymal spread of tumor in the liver (median survival 30 days, $n = 10$). In contrast, the treated animals survived longer than untreated controls (49 days, $n = 9$) ($P = 0.002$ versus untreated mice by the Mantel-Haenszel test, statistically significant at α level of $0.05/6 = 0.0083$ after Bonferroni correction for multiple comparisons). Single or multiple injections (once a week to a total of four injections) of c-SF-25-LAK cells beginning at 14 days after the tumor cell injection (when there are macrometastases in the liver) improved the survival rate of the mice (single injection, 45 days, $n = 9$, $P = 0.034$ versus untreated mice; and multiple injections, 54 days, $n = 4$, $P = 0.006$ versus untreated mice).

Under our experimental conditions, however, the in vivo purging of tumor cells by c-SF-25-LAK was not perfect. Therefore, the expression of SF-25 antigen in the tumors from mice treated with c-SF-25-LAK cells was examined to investigate whether treatment selected for the growth of tumor cells that no longer bore the SF-25 antigen. The SF-25 antigen was expressed in c-SF-25-LAK–treated tumor cells, as shown by histological examination (Fig. 4A) as well as by flow cytometry (Fig. 4B). Furthermore, LS 180 cells derived from both c-SF-25-LAK–treated and untreated mice were lysed by LAK cells in vitro. Therefore, the outgrowth of tumor in treated mice was not the result of selection of SF-25–negative or LAK-resistant tumor cells but may have resulted from an insufficient dose of c-SF-25-LAK for the tumor burden.

Adoptive immunotherapy using tumor-infiltrating lymphocytes (TILs) cultured with IL-2 has been reported to be more effective than LAK immunotherapy with respect to tumor response rates (*22*). TILs contain tumor-specific T lymphocytes (*23*). The cellular basis for successful adoptive immunotherapy of tumors by TIL may relate to the ability of tumor-specific T cells to traffic to and target tumor cells in vivo (*24*). Human TILs, but not human LAK cells (*4*), have been shown to immunolocalize to tumors in vivo (*24*). The present studies demonstrate the ability of MAb-directed human LAK cells to inhibit the growth of human colon cancer established in the liver of SCID mice. Because no increased cytotoxicity was observed in c-SF-25-LAK cells as compared with LAK cells alone in vitro, this augmentation of the anti-tumor effect must be largely due to the specific targeting of LAK cells to the

tumor mass rather than the cytotoxicity induced by an ADCC mechanism (25). We conclude that the targeting of human LAK cells to colon tumors is an important factor in the inhibition of tumor growth in vivo and that the SCID mouse–human xenogeneic chimeric model is useful for the study of anti-tumor properties of human effector cells. As demonstrated by the results of the present studies, it will be possible to test genetically modified human effector cells by conjugating the cells with tumor-specific antibodies to further increase their anti-tumor effects (26).

REFERENCES AND NOTES

1. E. A. Grimm, A. Mazumder, H. Z. Zhang, S. A. Rosenberg, *J. Exp. Med.* **155**, 1823 (1982); J. H. Phillips and L. L. Lanier, *ibid.* **164**, 814 (1986).
2. S. A. Rosenberg *et al.*, *N. Engl. J. Med.* **313**, 1485 (1985); W. H. West *et al.*, *ibid.* **316**, 898 (1987).
3. I. Kawase *et al.*, *Cancer Res.* **48**, 1173 (1988).
4. B. Mukherji *et al.*, *Int. J. Radiat. Appl. Instrum. B* **15**, 419 (1988).
5. G. C. Bosma, R. P. Custer, M. J. Bosma, *Nature* **301**, 527 (1983); M. J. Bosma and A. M. Carroll, *Annu. Rev. Immunol.* **9**, 323 (1991).
6. D. E. Mosier, R. J. Gulizia, S. M. Baird, D. B. Wilson, *Nature* **335**, 256 (1988); J. M. McCune *et al.*, *Science* **241**, 1632 (1988); R. B. Bankert *et al.*, *Curr. Top. Microbiol. Immunol.* **152**, 201 (1989); K. Pfeffer, K. Heeg, R. Bubeck, P. Conradt, H. Wagner, *ibid.*, p. 212; E. Simpson, J. Farrant, P. Chandler, *Immunol. Rev.* **124**, 97 (1991).
7. I. G. H. Schmidt-Wolf, R. S. Negrin, H.-P. Kiem, K. G. Blume, I. L. Weissman, *J. Exp. Med.* **174**, 139 (1991).
8. H. Takahashi *et al.*, *Gastroenterology* **96**, 1317 (1989).
9. The SCID–human colon cancer model was established according to the method described in (*8*), with modification. SCID mice anesthetized by intraperitoneal injection of 2% chloral hydrate (0.4 ml per mouse) were injected with 10^6 LS 180 cells and 20 μg of rabbit antibodies to asialo G_{M1} (Wako) in 0.25 ml of PBS (injection into the portal vein via splenic hilus with a 27-gauge needle). After 1 min, the portal vein was ligated and the spleen removed.
10. I. J. Fidler, *Cancer Res.* **50**, 6130 (1990).
11. H. Nelson, *Cancer Cells* **3**, 163 (1991).
12. B. Wilson *et al.*, *Proc. Natl. Acad. Sci. U.S.A.* **85**, 3140 (1988); H. Takahashi *et al.*, *Cancer Res.* **48**, 6573 (1988).
13. H. Takahashi, unpublished data.
14. K. Dorshkind, S. B. Pollack, M. J. Bosma, R. A. Phillips, *J. Immunol.* **134**, 3798 (1985); G. J. Bancroft, R. D. Schreiber, E. R. Unanue, *Immunol. Rev.* **124**, 5 (1991).
15. D. Herlyn and H. Koprowski, *Proc. Natl. Acad. Sci. U.S.A.* **79**, 4761 (1982); Z. Steplewski *et al.*, *ibid.* **85**, 4852 (1988); W. J. Johnson *et al.*, *J. Immunol.* **136**, 4704 (1986).
16. J. F. Jones and D. M. Segal, *J. Immunol.* **125**, 926 (1980).
17. MAb c-SF-25 was produced and provided by Centocor Inc. (Malvern, PA). We constructed a human-mouse chimeric Ig gene by joining variable region genes of light and heavy chains isolated from MAb SF-25 hybridoma cells to constant region genes of human κ light and γ 1 heavy chains. This construct was then transfected into Sp2/0 myeloma cells to produce the chimeric MAb.
18. J. R. Ortaldo, A. Mason, R. Overton, *J. Exp. Med.* **164**, 1193 (1986); K. Roberts, M. T. Lotze, S. A. Rosenberg, *Cancer Res.* **47**, 4366 (1987).
19. J. C. Unkeless, *J. Clin. Invest.* **83**, 355 (1989); J. V. Ravetch and J. P. Kinet, *Annu. Rev. Immunol.* **9**, 457 (1991).
20. LAK cells were incubated with MAb c-SF-25 (2 mg/ml) in RPMI 1640 for 30 min at 4°C. An equal volume of 30% PEG 8000 (Sigma) in RPMI 1640 was added to this cell mixture and incubated for an additional 90 min at 4°C. Finally, the cells were washed with PBS three times. As a control, human LAK cells were incubated with MAb c-SF-25 (2 mg/ml) for 90 min at 4°C and washed three times.
21. E. Vivier *et al.*, *J. Immunol.* **146**, 206 (1991).
22. S. A. Rosenberg *et al.*, *N. Engl. J. Med.* **319**, 1676 (1988).
23. J. T. Kurnick, R. L. Kradin, R. Blumberg, E. E. Schneeberger, L. A. Boyle, *Clin. Immunol. Immunopathol.* **38**, 357 (1986); L. M. Muul, P. J. Spiess, E. P. Director, S. A. Rosenberg, *J. Immunol.* **138**, 989 (1987).
24. B. Fisher *et al.*, *J. Clin. Oncol.* **7**, 250 (1989); K. D. Griffith *et al.*, *J. Natl. Cancer Inst.* **81**, 1709 (1989).
25. R. J. Dearman *et al.*, *Blood* **72**, 1985 (1988); A. W. Tong, J. C. Lee, R.-M. Wang, G. Ordonez, M. J. Stone, *Cancer Res.* **49**, 4103 (1989).
26. K. Nishihara *et al.*, *Cancer Res.* **48**, 4730 (1988); S. A. Rosenberg *et al.*, *N. Engl. J. Med.* **323**, 570 (1990); T. Friedmann, *Cancer Cells* **3**, 271 (1991).

27. Supported by grants CA-57584 and CA-35711 from the National Institutes of Health. We thank J. R. Wands and K. J. Isselbacher for review of the manuscript and for advice and support and R. Carlson and M. Nakaki for assistance.

2 October 1992; accepted 17 December 1992

Optical Time-of-Flight and Absorbance Imaging of Biologic Media

David A. Benaron and David K. Stevenson

Imaging the interior of living bodies with light may assist in the diagnosis and treatment of a number of clinical problems, which include the early detection of tumors and hypoxic cerebral injury. An existing picosecond time-of-flight and absorbance (TOFA) optical system has been used to image a model biologic system and a rat. Model measurements confirmed TOFA principles in systems with a high degree of photon scattering; rat images, which were constructed from the variable time delays experienced by a fixed fraction of early-arriving transmitted photons, revealed identifiable internal structure. A combination of light-based quantitative measurement and TOFA localization may have applications in continuous, noninvasive monitoring for structural imaging and spatial chemometric analysis in humans.

The principles that underlie the imaging of the interior of living bodies with light have application to a variety of situations that involve radiation transmission through opaque scattering media. Images can be formed with x-ray tomography (*1*), magnetic resonance (*2*), ultrasound (*3*), positron emission (*4*), thermal emission (*5*), electrical impedance (*6*), and other probes; but these have drawbacks that limit their use in the continuous, noninvasive monitoring of humans (*7*). Light, on the other hand, is nonionizing, relatively safe, and known to function well as a medical probe (*8–13*). In particular, red and near-infrared light pass easily through structures such as the skull (*9*), penetrate deeply into many tissues (*10*), are well tolerated in large doses (*11*), and can be used to quantitate chemical concentrations if an optical path length is known or estimated (*12*).

Variations in tissue absorbance and scattering over space and time influence photon travel through tissue. For example, breast tumors often attenuate light to a greater degree than neighboring tissues, possibly because of the presence of numerous blood vessels and mitochondria (*11, 13*). Spatial variations in absorbance have been used to form transillumination "shadowgrams" of such tumors (*13*), to detect cerebral bleeding (*14*), and to reconstruct two-dimensional steady-state tomographs (*15*). Temporal variations in absorbance, which can be caused by optical changes in certain proteins as oxygen pressure varies (*16*), have been used to estimate changes in the oxygenation of the brain (*8, 12, 17*) and extremities (*18*) and to measure blood flow and volume in tissues (*19*). Spectral analysis may also permit in vivo quantitation of substances such as glucose and cholesterol (*20*).

Optical imaging (*7*) and spectroscopy (*20*) in vivo have been difficult. With conventional radiological methods, photon scattering is minimal and, therefore, radiation travel is linear. In contrast, light takes highly irregular, diffusive paths through tissue, degrading image quality; detail is lost much as it is with distance in a fog. Scattering is the major attenuator of the intensity of transmitted photons in tissue (*21*). On average, a photon travels only millimeters into tissue, or less, before it scatters (*22*). Multiple scattering events occur for virtually all photons that propagate through tissue (*22, 23*), which causes them to take a wide range of paths as they traverse the tissue, each requiring a different amount of time. Because path lengths vary with absorbance and scattering, they are difficult to predict (*12*).

Medical Spectroscopy and Imaging Laboratory Section, Neonatal and Developmental Biology Laboratory, Department of Pediatrics, Stanford University School of Medicine, Palo Alto, CA 94305.